

# Can energy landscape roughness of proteins and RNA be measured by using mechanical unfolding experiments?

Changbong Hyeon and D. Thirumalai<sup>†</sup>

Chemical Physics Program, Institute for Physical Science and Technology, University of Maryland, College Park, MD 20742

Edited by Harold A. Scheraga, Cornell University, Ithaca, NY, and approved July 9, 2003 (received for review May 30, 2003)

**By considering temperature effects on the mechanical unfolding rates of proteins and RNA, whose energy landscape is rugged, the question posed in the title is answered in the affirmative. Adopting a theory by Zwanzig [Zwanzig, R. (1988) *Proc. Natl. Acad. Sci. USA* 85, 2029–2030], we show that, because of roughness characterized by an energy scale  $\varepsilon$ , the unfolding rate at constant force is retarded. Similarly, in nonequilibrium experiments done at constant loading rates, the most probable unfolding force increases because of energy landscape roughness. The effects are dramatic at low temperatures. Our analysis suggests that, by using temperature as a variable in mechanical unfolding experiments of proteins and RNA, the ruggedness energy scale  $\varepsilon$ , can be directly measured.**

Visualizing folding of proteins (1–3) and RNA (2) in terms of the underlying energy landscape has been fruitful in anticipating diverse folding scenarios. The polymeric nature of these biomolecules and the presence of multiple energy scales associated with the building blocks of proteins and RNA make their underlying energy landscape rugged. By rugged, we mean that the energy landscape consists of several minima separated by barriers of varying heights. To understand the diversity of the folding pathways, it is necessary to determine the characteristics of the energy landscape experimentally.

It is difficult to represent the large dimensional space of the energy landscape in terms of a few parameters. However, the ruggedness of the energy landscape can be described in terms of an energy scale  $\varepsilon$  regardless of the precise nature of the underlying reaction coordinate. Within the energy landscape picture, it is clear that rapid folding to the native conformation on a finite (biologically relevant) time scale is unlikely if  $\varepsilon/k_B T \gg 1$  ( $k_B$  is the Boltzmann constant, and  $T$  is the temperature) (1). Folding of proteins and RNA for which  $\varepsilon/k_B T \gg 1$  is, therefore, dominated by kinetic traps.

There are a number of proteins that fold kinetically in an apparent “two-state” manner (4). Similarly, tRNA and independently folding subdomains of large RNA (for example, the P5abc construct of *Tetrahymena thermophila* Group I intron) are also predicted to follow “two-state” kinetics (2). However, due to the polymeric nature of proteins and RNA, there is inherent incompatibility between local structures ( $\alpha$ -helical  $\beta$ -strands in protein and helical “secondary” structures in RNA) and the global folds that results in topological frustration (2) even for “two-state” folders. Length scale-dependent ruggedness in the free energy landscape arises due to topological frustration. For “two-state” folders, the roughness arising from the presence of multiple energetic interactions is likely to be small i.e.,  $\varepsilon/k_B T \sim O(1)$ . By  $O(1)$ , we mean  $0 < \varepsilon/k_B T < 5$ . Although no direct measurement of  $\varepsilon$  has been made for biomolecules, it has been inferred by using a diffusion limited time scale for loop closure in model peptides, that  $\varepsilon/k_B T \approx 2$  (5).

The purpose of this paper is to show that mechanical unfolding experiments can be used to extract  $\varepsilon$ . The stretching of proteins (6–10) and, more recently, RNA (11–13) already has begun to provide glimpses of their underlying energy landscape. In concert with theoretical studies (9, 14, 15), these measurements can

be used to construct the free energy landscape of proteins and RNA. For example, we have shown that, by using dynamics of nonequilibrium stretching experiments, one can infer the distribution of free energy barriers in the absence of force (16). Measurement of distribution of free energy barriers requires following time-dependent events, at the single molecule level, when unfolding is induced by force. At present, laser optical tweezer and atomic force microscopy methods can measure force( $f$ )–extension( $z$ ) ( $f - z$ ) curves either at constant  $f$  or as a function of loading rates. We show here that, by using such experiments,  $\varepsilon$  can be directly measured if the force-dependent unfolding rates can be measured over a range of temperatures.

## Caricature of Energy Landscape of RNA and Proteins

We consider proteins and RNA that fold and unfold by an apparent “two-state” transition. Thus, the conformations of the biological molecules belong either to the native basin of attraction (NBA) or the unfolded basin of attraction (UBA). To describe the effect of force on RNA and proteins, we assume that the reaction  $UBA \rightleftharpoons NBA$  may be described by using a suitable low-dimensional reaction coordinate. Although the reduction of a multidimensional free energy landscape into one (or two) dimensions is a major simplification, it has been shown that such a description gives nearly quantitative results for a folding rate of minimally frustrated sequences (17). When subject to force, the 1D parameter, namely the extension of the molecule, is a natural reaction coordinate.

The free energy profile for  $UBA \rightleftharpoons NBA$  in terms of the scalar reaction coordinate,  $x$ , is taken to be “smooth” on long (18) (greater than the persistence length of the polypeptide or polynucleotide) length scales. As stated in the Introduction, we expect that for “two-state” folders, because of topological frustration, a scale-dependent roughness is superimposed on the overall smooth free energy landscape. Following Zwanzig (18), we assume that the length scale for roughness is  $\Delta x \ll R_g$  ( $R_g$  is the dimension of RNA or protein of interest), and the overall energy scale of roughness is  $\varepsilon$ . Thus, on length scales comparable to  $\Delta x$ , there are free energy barriers with typical barrier heights on the order of  $\varepsilon$  (Fig. 1). Our calculations are valid only when  $\varepsilon/\Delta F^\ddagger < 1$  ( $\Delta F^\ddagger$  is the average barrier height separating UBA from NBA). Zwanzig (18) showed that diffusion in such a rough landscape can be extremely slow, especially at low temperatures, even for modest values of  $\varepsilon$ . Here, we extend these calculations in the presence of applied force to show that  $\varepsilon$  can be measured by using single molecule pulling experiments.

## Unfolding at Constant Force

The energy landscape (see Fig. 1 for a caricature) can be decomposed into a smooth part  $F_0(x)$ , on which is superimposed the roughness  $F_1(x)$ . If a suitable 1D reaction coordinate can

This paper was submitted directly (Track II) to the PNAS office.

Abbreviations: NBA, native basin of attraction; UBA, unfolded basin of attraction.

<sup>†</sup>To whom correspondence should be addressed. E-mail: thirum@glue.umd.edu.

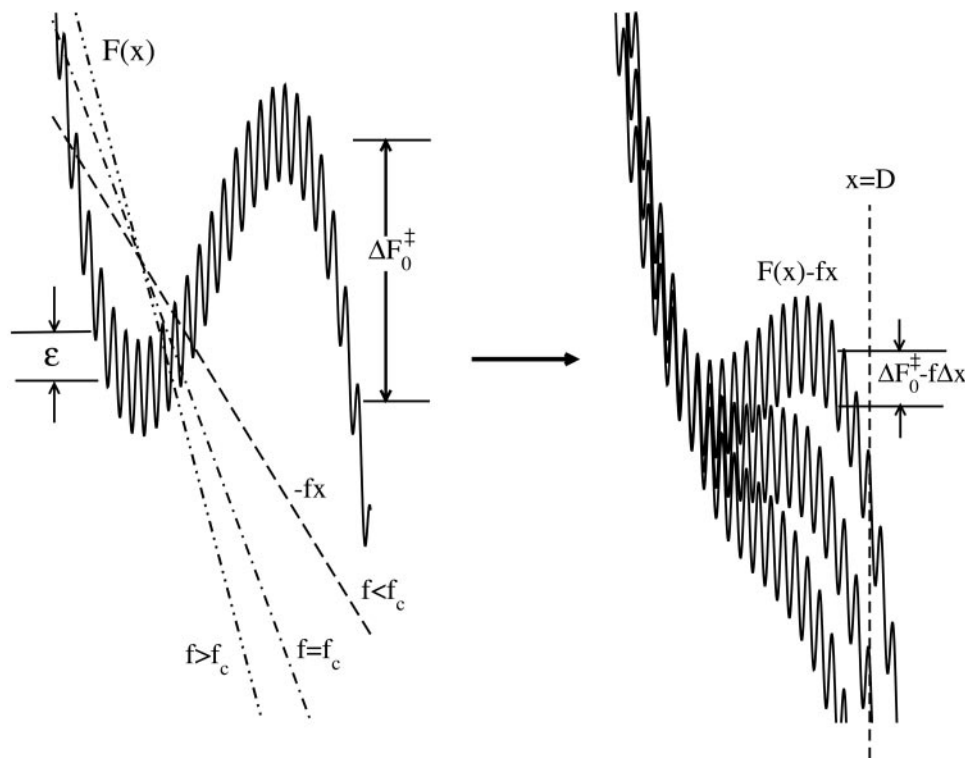


**Fig 1.** Caricature of the rough energy landscape of “two-state” proteins and RNA by using  $x$ , the coordinate that couples to force  $f$ , as the reaction constant. For clarity, we have represented the  $U$  state by an unbounded potential. The graph (Left) shows that on a long length scale, the landscape is smooth, whereas on short length scales, there are a number of barriers. We used  $F(x) = F_0(x) + F_1(x) = -Ax(x - p)(x + p) + \varepsilon \cos 2\pi qx$  to generate the rugged energy landscape. The parameters in the potential are  $A = 1 \text{ pN/nm}^2$ ,  $p = 5 \text{ nm}$ ,  $\varepsilon = 3.0 \text{ pN}\cdot\text{nm}$ ,  $q = 2.0 \text{ nm}^{-1}$ . The random variables  $\varepsilon$  and  $q$  are assumed to be given by Gaussian distribution with dispersions  $\sigma_q = 0.5 \text{ nm}^{-1}$  and  $\sigma_\varepsilon = 0.5 \text{ pN}\cdot\text{nm}$ . On application of force, [shown as  $-fx$  (Left)], the landscape is deformed (see Right). The extent of tilting depends on the precise value of force. The tilted potential, along with changes in the mean barriers, is shown for three values,  $f < f_c$ ,  $f = f_c$ , and  $f > f_c$ , where  $f_c$ , the critical value of force, is 25 pN for the chosen parameters.

describe mechanical unfolding of RNA and proteins, the force-dependent unfolding rate can be obtained by solving Kramer’s problem in the overdamped limit. Accordingly, we assume that diffusion in such an energy landscape is described by the Smoluchowski equation. The objective is to compute the mean first passage time (mfpt),  $\langle t, x \rangle$ , for transition from NBA to UBA in the presence of force. The mfpt  $\langle t, x \rangle$  is the mean time for reaching  $x$  starting from  $x_0$ . Assuming a reflecting barrier at  $a$  ( $a < x_0 < x$ ), Zwanzig (18) showed (see also ref. 19) that

$$\langle t, x \rangle \cong \int_{x_0}^x dy e^{\beta F_0(y) + \psi^+(y)} \frac{1}{D} \int_a^y dz e^{-\beta F_0(z) + \psi^-(z)}, \quad [1]$$

where  $D$  is the bare diffusion constant,  $\beta = 1/k_B T$ , and  $e^{\psi^\pm(z)} \equiv \langle e^{\pm \beta F_1(z)} \rangle$ , where  $\langle \dots \rangle$  is the spatial average of  $F_1(z)$  over the length scale  $\Delta z$ . The structure of the equation for  $\langle t, x \rangle$  suggests that there exists an effective Smoluchowski equation (18),

$$\frac{\partial}{\partial t} \rho(x, t) = \frac{\partial}{\partial x} D^*(x) e^{-\beta F^*(x)} \frac{\partial}{\partial x} e^{\beta F^*(x)} \rho(x, t), \quad [2]$$

that describes diffusion in a spatially averaged potential  $F^*(x) = F_0(x) - k_B T \psi^-(x)$ . In Eq. 2,  $\rho(x, t)$  is the probability distribution function, and  $D^*(x) = e^{-\psi^-(x)} D e^{-\psi^-(x)}$  is the spatially averaged effective diffusion constant. Assuming Eq. 2 is valid, we wish to solve Kramer’s problem (20) (computation of the unfolding rate of the native state) on application of  $f$  for the energy landscape sketched in Fig. 1. For the analysis to make sense,  $\varepsilon/\Delta F^\ddagger < 1$ , where  $\Delta F^\ddagger = \Delta F_0^\ddagger - f\Delta x$  is the value of the mean barrier (Fig. 1) that separates UBA from NBA. The inequality  $\varepsilon/\Delta F^\ddagger < 1$  will

ensure that the biomolecule of interest would fold in an apparent two-state manner when  $f = 0$ . When  $f \neq 0$ , the effective potential is  $F^*(x) = F_0(x) - fx - k_B T \psi^-$ . By expanding this potential around the minimum  $x_0$  and the transition state  $x_{ts}$  to quadratic order, the unfolding rate can be calculated by using Kramer’s theory. Let  $\omega_0$  be the frequency of the minimum around the NBA and  $\omega_{ts}$  be the frequency around the saddle point (the transition state). The unfolding rate is

$$k_R^{-1}(f) = \frac{2\pi\gamma}{\omega_0\omega_{ts}} \langle e^{-\beta F_1} \rangle \langle e^{\beta F_1} \rangle e^{\beta \Delta F_0^\ddagger - \beta f(x_{ts} - x_0)}, \quad [3]$$

where  $\Delta F_0^\ddagger = F_0(x_{ts}) - F_0(x_0)$ , and  $\gamma$  is the friction coefficient. It follows from Zwanzig’s analysis (18) that the effect of roughness manifests only in the renormalization of the effective diffusion constant. If we assume that the amplitude of roughness is independent of the position along the reaction coordinate, and that it is distributed as a Gaussian, then  $\langle e^{-\beta F_1} \rangle = \langle e^{\beta F_1} \rangle$ , so that

$$\log \left( \frac{k_R^{-1}(f)}{k_0^{-1}} \right) = \beta(\Delta F_0^\ddagger - f\Delta x) + \log \langle e^{\beta F_1} \rangle^2, \quad [4]$$

where  $k_0^{-1} = 2\pi\gamma/\omega_0\omega_{ts}$  and  $\Delta x = x_{ts} - x_0$ . The central result in Eq. 4 shows that roughness can lead to a non-Arrhenius temperature dependence in the mechanical unfolding rate. The result in Eq. 3 can also be extended to the case when there is memory in the friction, i.e., when  $\gamma$  is time dependent. The Kramer’s result for this case is  $k_R(f) = [(\hat{\gamma}^2(\lambda_0^{\text{ts}})/4 + \omega_{ts}^2)^{1/2} - \hat{\gamma}(\lambda_0^{\text{ts}})/2]/\omega_{ts} \omega_0/2\pi \langle e^{\beta F_1} \rangle^{-2} \exp(-\beta(\Delta F_0^\ddagger - f\Delta x))$ , where  $\hat{\gamma}$  is the Laplace transform of  $\gamma(t)$ , and  $\lambda_0^{\text{ts}}$  is the normal mode frequency

defined at the transition state (20). For weak roughness  $\beta F_1 < 1$ , we get

$$\log(k_R^{-1}(f)/k_0^{-1}) = \beta(\Delta F_0^\ddagger - f\Delta x) + \beta^2\langle F_1^2 \rangle, \quad [5]$$

which might be more useful in analyzing experiments.

### Stretching at a Constant Loading Rate

Mechanical unfolding experiments are typically performed far from equilibrium by stretching the ends of the molecule at a constant pulling speed. Large changes in the loading rate can be achieved by variations of the spring constant (related to the curvature of the optical trap potential in laser tweezer experiments) of the cantilever in atomic force microscopy (AFM). To fully probe the energy landscape of proteins and RNA, it is necessary to explore their response over a wide range of loading rates,  $r_f = df/dt = kv$  (21), where  $k$  is the spring constant of the cantilever, and  $v$  is the pulling speed. By using a combination of laser optical tweezer, bioforce membrane probes, and AFM, one can cover loading rates that vary by several orders of magnitude. In these experiments, the histogram of forces required to unfold the biomolecule is measured by stretching one molecule at a time.

The effect of roughness on the dependence of the most probable unfolding force on the loading rate,  $r_f$ , can be calculated by using Kramer's theory. Under a constant loading rate, the curvatures of the barrier  $\omega_{ts}$  as well as the barrier height change as  $f$  increases with time. The unfolding rate changes dynamically as (see Eq. 3)

$$k_R(f(t)) = \frac{\omega_0[f(t)]\omega_{ts}[f(t)]}{2\pi\gamma\langle e^{-\beta F_1} \rangle^2} e^{-\beta\{F_0(x_{ts}(f(t)) - F_0(x_0(f(t)))) + \beta f(t)(x_{ts}(f(t)) - x_0(f(t)))\}}. \quad [6]$$

The time-dependent probability of unfolding is  $P(t) = k(t)\exp(-\int_0^t d\tau k(\tau))$ . With  $r_f = df/dt$ , the distribution of forces for overcoming the barrier is

$$P(f) = \frac{1}{r_f} k_R(f) \exp\left(-\int_0^f df' \frac{1}{r_f} k_R(f')\right). \quad [7]$$

The most probable threshold force that drives unfolding is obtained by using  $dP(f)/df|_{f=f^*} = 0$ , which leads to

$$f^* = \frac{k_B T}{\Delta x(f^*)} \left\{ \log\left(\frac{r_f \Delta x(f^*)}{v_D(f^*) e^{-\beta \Delta F_0^\ddagger(f^*)} k_B T}\right) + \log\left(1 + f^* \frac{\Delta x'(f^*)}{\Delta x(f^*)} - \frac{(\Delta F_0^\ddagger)'(f^*)}{\Delta x(f^*)} + \frac{v_D'(f^*)}{v_D(f^*)} \frac{k_B T}{\Delta x(f^*)}\right) + \log\langle e^{\beta F_1} \rangle^2 \right\}, \quad [8]$$

where  $\Delta F_0^\ddagger(f) \equiv F_0(x_{ts}(f)) - F_0(x_0(f))$ , ' denotes differentiation with respect to the argument,  $\Delta x(f) \equiv x_{ts}(f) - x_0(f)$  is the distance between the transition and native states, and  $v_D(f) \equiv \omega_0(f)\omega_{ts}(f)/2\pi\gamma$ . If  $\Delta F_0(f)$ ,  $\Delta x(f)$ , and the intrinsic angular frequency at the top and bottom of the barrier are relatively insensitive to the change of force, the second term on the right-hand side of Eq. 8 would vanish, leading to  $f^* \propto (k_B T/\Delta x) \log r_f$  (21). However, if the loading rate spans a wide range, the resulting  $f^*$  can deviate substantially from the predicted logarithmic dependence on  $r_f$ .

It follows from Eq. 8 that the effect of roughness on  $f^*$  is similar to that shown in Eq. 4. As the extent of roughness increases, the value of  $f^*$  can increase substantially. To use Eq.

8 to estimate  $\langle e^{\beta F_1} \rangle^2$  shifts in  $f^*$  due to roughness must exceed the dispersions in  $P(f)$  when  $\varepsilon \approx 0$ .

### Numerical Results

The theory presented here shows that, by using constant force mechanical unfolding experiments, the magnitude of roughness can be measured if temperature can be varied. Our central result has been derived by assuming that, in the presence of force, the Smoluchowski equation (Eq. 2) is valid for the roughness averaged potential. To test the validity of this assumption, we have performed Monte Carlo simulations for a model potential  $F(x) = F_0(x) + F_1(x) = -Ax(x-p)(x+p) - f(x+p/\sqrt{3}) + \varepsilon \cos(2\pi qx)$ . The strength of the random potential  $\varepsilon$  and its range  $q^{-1}$  are taken from a Gaussian distribution with zero mean. For this potential, with the parameters given in the legend to Fig. 1, we calculated the mean unfolding time for a number of realizations of the random potential. The mean unfolding time is computed from the histogram of the first passage time, which is the first time the particle reaches the boundary at  $x = D = 1.5p$ . For a given force, the mean first passage time is computed as a function of temperature in the range of  $3.80 \text{ pN} \cdot \text{nm} \leq k_B T \leq 4.50 \text{ pN} \cdot \text{nm}$ . The numerical simulations were performed by using the smart Monte Carlo algorithm (22) with parameters,  $\gamma = 4.14 \times 10^{-8} \text{ pN} \cdot \text{sec/nm}$ , and time step,  $dt = 2.0 \times 10^{-10} \text{ sec}$ .

In accord with our prediction (Eq. 4), we find that the numerically computed logarithm of mfpt,  $\log \tau$ , as a function of  $k_B T$  for the three values of  $f$ , can be fit as  $\log \tau = a + b/k_B T + c/k_B^2 T^2$  (Fig. 2). If the theoretical prediction is valid, we expect that the value of  $c = \varepsilon^2$ , which for our model is  $\varepsilon^2 = 9.0 \text{ pN}^2 \cdot \text{nm}^2$  independent of  $f$ . We have used Eq. 5 instead of Eq. 4 because the value of  $\varepsilon$  is less than the temperature used in the simulation, i.e.,  $\varepsilon/k_B T \sim O(1)$ . The numerical fits give  $\varepsilon^2 = 9.9, 9.9, \text{ and } 8.9$  for  $15 \text{ pN} (< f_c), 25 \text{ pN} (= f_c), 40 \text{ pN} (> f_c)$ , respectively. The critical force  $f_c$  for our choice of parameters is  $25 \text{ pN}$ . The coefficient  $b = \beta(\Delta F_0^\ddagger - f\Delta x)$  should be equal to  $24.3, 0.0, 0.0$  for  $15 \text{ pN} (< f_c), 25 \text{ pN} (= f_c), \text{ and } 40 \text{ pN} (> f_c)$ . The fits give  $b = 23.4, 0.9, \text{ and } -0.8$ , respectively. Thus, the numerical results confirm the validity of Eq. 5 in the limit when the roughness is small. If  $\varepsilon/k_B T \gg 1$ , the temperature dependence of force-induced unfolding would have significant curvature, as can be seen by a cumulant expansion of  $\log\langle e^{\beta F_1} \rangle^2$  (Eq. 4).

### Proposed Experiments

The theoretical considerations presented here allow us to propose mechanical unfolding experiments that can be used to measure a key statistical characteristic of the energy landscape of proteins and RNA, namely the roughness scale  $\varepsilon$ . Measurements of the unfolding rates as a function of temperature with the force held constant can be used to estimate  $\varepsilon$  (Eqs. 3 and 5). There is a significant advantage in the proposed experiments to measure  $\varepsilon$ . If the theoretical predictions hold good, measurements of  $\varepsilon$  with single-molecule mechanical unfolding experiments would not involve any assumption about the underlying folding reaction coordinates. Moreover, no modeling about the dynamics of proteins and RNA is required to extract  $\varepsilon$  from mechanical unfolding experiments.

Using Eqs. 3 and 4 to measure  $\varepsilon$  is most efficacious if temperature variation of  $k_0^{-1}$  does not compromise the signal arising from the third term in Eq. 4 or Eq. 5. Because  $k_0^{-1} \propto \eta$ , the viscosity of the solution, corrections due to variations of  $\eta$  with respect to  $T$ , have to be taken into account in using Eq. 3 to analyze experiments. The variable temperature range in mechanical unfolding experiments is likely to be  $5^\circ\text{C} < T < 50^\circ\text{C}$ . Over this temperature range,  $\eta$  for water varies as  $\exp(A/T)$  (23). As a result, the coefficient of the  $1/T^2$  term in  $\log k_R^{-1}(f)$  can be estimated by using mechanical unfolding experiments.

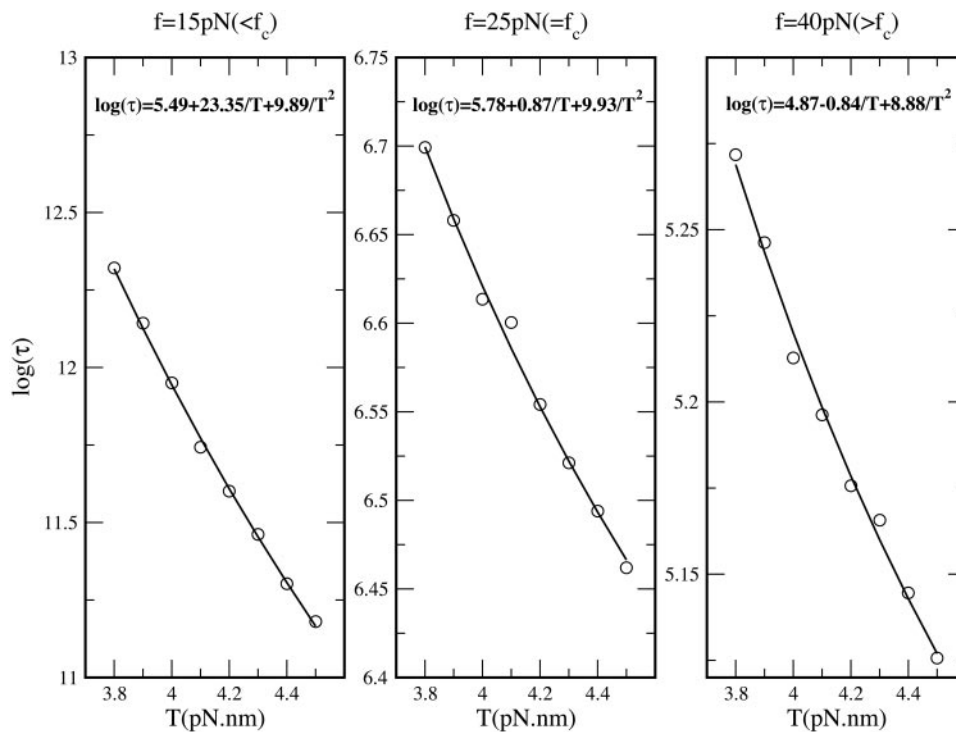


**Fig 2.** The logarithm of the mean first passage time,  $\log \langle \tau \rangle$  as a function of temperature at three values of  $f$ . The symbols are numerical results, and the lines are for using  $\log \langle \tau \rangle = a + b/T + c/T^2$  (Eq. 5).

Let us consider how to use mechanical unfolding experiments at a constant loading rate to obtain  $\varepsilon$ . A straightforward application of Eq. 8 to measure  $\varepsilon$  is difficult, because a number of

variables in Eq. 8 are functions of  $f^*$ . A plausible way of using Eq. 8 to estimate  $\varepsilon$  is illustrated in Fig. 3, which shows  $P(f)$  and  $f^*$  as a function of the loading rate at two different temperatures. By

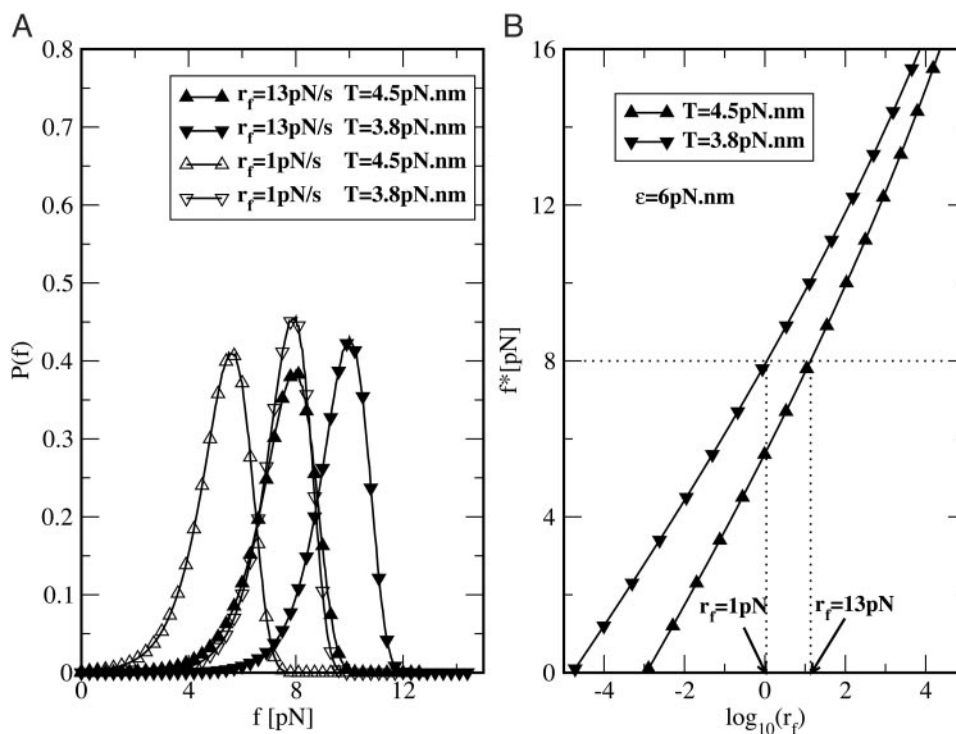


**Fig 3.** (A) Distribution of unfolding forces  $P(f)$  at two temperatures and two loading rates for the potential described in the Fig. 1 legend. The parameters are the same as in Fig. 2. (B) Dependence of  $f^*$ , the most probable unfolding force, as a function of the loading rate  $r_f$  at two temperatures. The curvature in the lines indicates deviations from  $f \propto \ln r_f$ . The procedure to extract  $\varepsilon$  from these curves is described in the text.

using such 2D experiments (done by varying  $r_f$  and  $T$ ), one can obtain the values of  $r_f$  that give rise to identical  $f^*$  value at two temperatures. The measured  $r_f$  values at temperature  $T_1$  and  $T_2$  allow us to estimate  $\varepsilon^2$  (for small  $\varepsilon/k_B T$ ) with

$$\varepsilon^2 \approx \frac{k_B T_2 \times k_B T_1}{k_B T_2 - k_B T_1} \cdot \left( k_B T_1 \log \frac{r_f(T_1) \Delta x(f^*)}{\nu_D(f^*) k_B T_1} - k_B T_2 \log \frac{r_f(T_2) \Delta x(f^*)}{\nu_D(f^*) k_B T_2} \right). \quad [9]$$

In obtaining Eq. 9, we have assumed that the second term in Eq. 8 is small. The numerical results (Fig. 3) for the energy landscape in Fig. 1 show that the separation in  $f^*$  as a function of temperature is greater at smaller loading rates that are easily accessible in laser optical tweezer experiments. Moreover, the dispersion in  $P(f)$  is also smaller at smaller loading rates. These

calculations show that measurements of  $f^*(r_f, T)$  with optical tweezer experiments can be used to measure  $\varepsilon^2$  by using Eq. 9.

## Conclusion

We have shown that including temperature as a variable in mechanical unfolding experiments can yield valuable quantitative measurements of the characteristics of the energy landscape of proteins and RNA without any assumption about their dynamics. In our previous studies (16), we had shown that the phase diagram in the  $(f, T)$  plane of protein can reveal many features about intermediates in the folding/unfolding problem. Previous theoretical studies (9, 14, 15) and the present work show that variable temperature mechanical unfolding experiments have great potential in probing the energy landscape of biomolecules at the single-molecule level.

We thank C. Bustamante for a useful conversation. We are grateful to R. I. Dima, D. K. Klimov, and M. S. Li for a careful reading of the paper. This work was supported in part by National Science Foundation Grant NSF029340.

1. Bryngelson, J. D., Onuchic, J. N., Socci, N. D. & Wolynes, P. G. (1995) *Protein Struct. Funct. Genet.* **21**, 167–195.
2. Thirumalai, D. & Woodson, S. A. (1996) *Acc. Chem. Res.* **29**, 433–439.
3. Dill, K. A. & Chan, H. S. (1997) *Nat. Struct. Biol.* **4**, 10–19.
4. Jackson, S. E. (1998) *Folding Des.* **3**, R81–R91.
5. Lapidus, L. J., Eaton, W. A. & Hofrichter, J. (2000) *Proc. Natl. Acad. Sci. USA* **97**, 7220–7225.
6. Kellermeier, M. Z., Smith, S. B., Granzier, H. L. & Bustamante, C. (1997) *Science* **276**, 1112–1116.
7. Tskhovrebova, L., Trinick, J., Sleep, J. A. & Simmons, R. M. (1997) *Nature* **387**, 308–312.
8. Reif, M., Gautel, H., Oesterhelt, F., Fernandez, J. M. & Gaub, H. E. (1999) *Science* **276**, 1109–1112.
9. Isralewitz, B., Gao, M. & Schulten, K. (2001) *Curr. Opin. Struct. Biol.* **11**, 224–230.
10. Zhuang, X. & Reif, M. (2003) *Curr. Opin. Struct. Biol.* **13**, 86–97.
11. Liphardt, J., Onoa, B., Smith, S. B., Tinoco, I. & Bustamante, C. (2001) *Science* **292**, 733–737.
12. Liphardt, J., Dumont, S., Smith, S. B., Tinoco, I. & Bustamante, C. (2002) *Science* **296**, 1832–1835.
13. Onoa, B., Dumont, S., Liphardt, J., Smith, S. B., Tinoco, I. & Bustamante, C. (2003) *Science* **299**, 1892–1895.
14. Hummer, G. & Szabo, A. (2001) *Proc. Natl. Acad. Sci. USA* **98**, 3658–3661.
15. Klimov, D. K. & Thirumalai, D. (2000) *Proc. Natl. Acad. Sci. USA* **97**, 7254–7259.
16. Klimov, D. K. & Thirumalai, D. (2001) *J. Phys. Chem. B* **105**, 6648–6654.
17. Nymeyer, H., Socci, N. D. & Onuchic, J. N. (2000) *Proc. Natl. Acad. Sci. USA* **97**, 634–639.
18. Zwanzig, R. (1988) *Proc. Natl. Acad. Sci. USA* **85**, 2029–2030.
19. Lifson, S. & Jackson, J. L. (1962) *J. Chem. Phys.* **36**, 2410–2414.
20. Hanggi, P., Talkner, P. & Borkovec, M. (1990) *Rev. Mod. Phys.* **62**, 251–341.
21. Evans, E. & Ritchie, K. (1997) *Biophys. J.* **72**, 1541–1555.
22. Rossky, P. J., Doll, J. D. & Friedman, H. L. (1978) *J. Chem. Phys.* **69**, 4628–4633.
23. Lide, D. R. (1995) *Handbook of Chemistry and Physics* (CRC Press, Boca Raton, FL), 76th Ed.